**Atmospheric
Chemistry
and Physics**

Using a photochemical model for the validation of NO_2 satellite measurements at different solar zenith angles

A. Bracher, M. Sinnhuber, A. Rozanov, and J. P. Burrows

Institute of Environmental Physics and Remote Sensing (IUP/IFE), University of Bremen, Otto-Hahn-Allee 1, 28334 Bremen, Germany

Abstract. SCIAMACHY (Scanning Imaging Spectrometer for Atmospheric Chartography) aboard the recently launched Environmental Satellite (ENVISAT) of ESA is measuring solar radiance upwelling from the atmosphere and the extraterrestrial irradiance. Appropriate inversion of the ultraviolet and visible radiance measurements, observed from the atmospheric limb, yields profiles of nitrogen dioxide, NO_2, in the stratosphere (SCIAMACHY-IUP NO_2 profiles V1). In order to assess their accuracy, the resulting NO_2 profiles have been compared with those retrieved from the space borne occultation instruments Halogen Occultation Experiment (HALOE, data version v19) and Stratospheric Aerosol and Gas Experiment II (SAGE II, data version 6.2). As the HALOE and SAGE II measurements are performed during local sunrise or sunset and because NO_2 has a significant diurnal variability, the NO_2 profiles derived from HALOE and SAGE II have been transformed to those predicted for the solar zenith angles of the SCIAMACHY measurement by using a 1-dimensional photochemical model. The model used to facilitate the comparison of the NO_2 profiles from the different satellite sensors is described and a sensitivity ananlysis provided. Comparisons between NO_2 profiles from SCIAMACHY and those from HALOE NO_2 but transformed to the SCIAMACHY solar zenith angle, for collocations from July to October 2002, show good agreement (within $+/-12\%$) between the altitude range from 22 to 33 km. The results from the comparison of all collocated NO_2 profiles from SCIAMACHY and those from SAGE II transformed to the SCIAMACHY solar zenith angle show a systematic negative bias of 10 to 35% between 20 km to 38 km with a small standard deviation between 5 to 14%. These results agree with those of Newchurch and Ayoub (2004), implying that above 20 km NO_2 profiles from SAGE II sunset are probably somewhat high.

Correspondence to: A. Bracher
(bracher@uni-bremen.de)

1 Introduction

Nitrogen dioxide, NO_2, plays a number of important roles in the chemistry of the stratosphere. It is not only involved in catalytic cycles leading to ozone, O_3, destruction, but also in processes, buffering chlorine activation and oxides of hydrogen through the formation of the temporary reservoir, such as chlorine nitrate, $ClONO_2$, (Brasseur and Solomon, 1986), Reservoir species like HO_2NO_2 and N_2O_5 have the property to remove reactive species like NO_2 for a certain time from fast reactions.

Gaseous peroxynitric acid (HO_2NO_2) is produced by the reaction:

$$NO_2 + HO_2 + M \rightarrow HO_2NO_2 + M \tag{R1}$$

While it is destroyed by photolysis and reaction with OH:

$$HO_2NO_2 + h\nu \rightarrow NO_2 + HO_2 \tag{R2}$$

$$HO_2NO_2 + OH \rightarrow H_2O + O_2 + NO_2, \tag{R3}$$
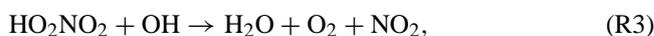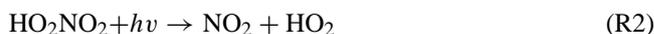
as well as by collisional decomposition which is the reverse reaction of (R1). Thus the molecule HO_2NO_2 is important in both nitrogen and hydrogen chemistry.

Dinitrogen pentoxide (N_2O_5) is formed during the night by the following reactions of NO_2 and NO_3:

$$NO_2 + O_3 \rightarrow NO_3 + O_2 \tag{R4}$$

$$NO_3 + NO_2 + M \rightarrow N_2O_5 + M \tag{R5}$$
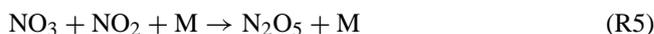
After sunrise, N_2O_5 photolyzes back into NO_2 and NO_3:

$$N_2O_5 + h\nu \rightarrow NO_2 + NO_3 \tag{R6}$$

It can also be destroyed by collisional decomposition which is the reverse reaction of (R5).

NO_2 photolyzes to form NO,

$$NO_2 + h\nu \rightarrow NO + O, \tag{R7}$$

and NO reacts with O$_3$ to reform NO$_2$

$$O_3 + NO \rightarrow NO_2 + O_2. \qquad (R8)$$

The behaviour of NO$_2$ in the stratosphere is largely controled by the above reactions, which result in a significant diurnal variation in NO$_2$ amount, with a minimum after sunrise and a maximum shortly after sunset (when NO is rapidly converted to NO$_2$). The partitioning of N$_2$O$_5$ also leads to a seasonal variation in NO$_2$ densities. During polar summer, the near-constant sunlight prevents buildup of NO$_3$ and hence precludes formation of N$_2$O$_5$. Thus, NO$_2$ densities are higher in the polar summer than in the winter, at which time more NO$_x$ is sequestered in the N$_2$O$_5$ reservoir (Solomon and Keys, 1992)

The short-lived radical NO$_2$ has been observed in the atmosphere since the 1970s by means of passive remote sensing in the ultraviolet and visible spectral regions from instrumentation either at the ground, or flown on aircraft, balloons, and spacecraft. Similarly, instruments aboard satellite platforms, aimed at retrieving NO$_2$ profiles, have also employed solar occultation: examples are the family of instruments known as the Stratospheric Aerosol and Gas Experiment (SAGE I, II, III; Chu and McCormick, 1979; Mauldin et al., 1985; NASA LaRC, 2004), the two instruments called Polar Ozone and Aerosol Measurements (POAM II, III; Glaccum et al., 1996; Lucke et al., 1999), the two Improved Limb Atmospheric Spectrometers (ILAS I, II; Sasano et al., 1999; Nakajima et al., 2004) and the Halogen Occultation Experiment (HALOE; Russell III et al., 1993). The sunsynchronous orbits of the satellites on which POAM, ILAS and SAGE III instruments are flown, result in solar occultation measurements only being possible at high latitudes. HALOE, SAGE I and SAGE II fly on platforms in asynchronous orbits and thereby achieve global coverage of solar occultation measurements within a year.

As explained above, the concentration of NO$_2$ in the stratosphere exhibits a significant diurnal cycle, measurements at a variety of solar zenith angles (SZA) are therefore required to improve our understanding of the chemistry and dynamics of NO$_2$ in the stratosphere. As early as 1980, NO and NO$_2$ were measured simultaneously in the stratosphere with a balloon-borne instrument, and the measured diurnal variability was shown to agree qualitatively well with model results (Roscoe et al., 1981). In the study by Payan et al. (1999) the balloon-borne instruments Limb Profile Monitor of the Atmosphere (LPMA) and the Absorption par Minoritaires Ozone et NO$_x$ (AMON) have been used to measure NO$_2$, during sunset and also 5 h later during night. In addition, since 1994 balloon flights of the Michelson Interferometer for Passive Atmospheric Sounding (MIPAS-B) have been undertaken for different geophysical conditions of the stratosphere. Vertical profiles of NO$_2$ are measured among the other major components of the nitrogen family at night, at sunrise and a few hours after sunrise (Stowasser et al., 2003). In addition to its solar occultation measurements, the SAGE

III instrument measures in lunar occultation mode, which enables to retrieve NO$_2$ profiles in the SZA range of between 95° and 115° (NASA LaRC, 2004).

SCIAMACHY (Scanning Imaging Absorption Spectrometer for Atmospheric Chartography, see e.g. Bovensmann et al., 1999), MIPAS (Michelson Interferometer for Passive Atmospheric Sounding, see e.g. Stiller et al., 2001) and GOMOS (Global Ozone Monitoring by Occultation of Stars, see e.g. Bertraux et al., 1991) are space-based atmospheric instruments launched on board ENVISAT (Environmental Satellite) in March 2002. These three atmospheric ENVISAT instruments provide information about a variety of trace gases, including NO$_2$ profiles. ENVISAT orbits the Earth 14 times per day in a polar sun-synchronous orbit with an inclination of 98.7° in a descending node and having an equator crossing time of 10:00 local solar time. This results in measurements being made at a range of SZAs, during day (MIPAS and solar occultation and limb measurements of SCIAMACHY), and night (MIPAS, GOMOS and during the time around local full moon SCIAMACHY lunar occultation). Global coverage of the limb sounding measurements is reached within less than six days.

In order to exploit fully the retrievals of NO$_2$ from the measurements made aboard ENVISAT, the relevant data products have to be validated. In addition to validation by comparison with balloon measurements, a validation with a collocated data set of a larger seasonal and global coverage is needed. The use of independent satellite measurements to validate trace gas products of the ENVISAT instruments has the great advantage that pole-to-pole coverage for all seasons is available and that validation activities are not restricted to a limited set of dates and locations. As a result, this study attempts to validate the NO$_2$ products V1 retrieved at the Institute of Environmental Physics from SCIAMACHY Level-0 limb data by comparisons with the established and well validated data products from satellite instruments HALOE (described in Russell III et al., 1993), and SAGE II (described in Mauldin et al., 1985).

As the NO$_2$ measurements from SAGE II and HALOE are performed during local sunrise or sunset, measurements made in space and time close to the ENVISAT measurements have to take into account appropriately the difference in the SZAs of the SCIAMACHY and the occultation instrument. Photochemical model studies of varying complexity have been used extensively in the past to investigate different aspects of trace gas measurements, and also to make measurements taken by different instruments, in different airmasses or at different SZAs comparable. Harder et al. (2003) compared modeled BrO profiles; in this case, the model was not constrained, but only measurements, where NO$_2$, O$_3$ and N$_2$O measured simultaneously to the BrO agreed well with model results, were chosen for the comparison. Stowasser et al. (2003) investigated the change of several NO$_y$ species at different SZAs by comparing measurements from the MIPAS-B to model results. In this case, also the

model was not constrained, and large differences between the modelled and measured individual NO$_y$ species were observed, but the HNO$_3$/NO$_y$, N$_2$O$_5$/NO$_y$, and NO$_2$/NO$_y$ ratios were found to be in good agreement over a large altitude range. Sinnhuber et al. (2002) use a combination of a global three-dimensional model with a one-dimensional model to intercompare ground-based measurements of BrO slant columns at different stations ranging from the Northern high latitudes over mid-latitudes and the tropics to Southern high latitudes. Vogel et al. (2003) compared measurements from a balloon-borne in-situ ClO/BrO instrument to model results; in this case, the model was initialised with measurements obtained several weeks earlier with another balloon-borne instrument. Marchand et al. (2003) have assimilated measurements of NO$_2$ and O$_3$ made during sunrise and sunset by a SAOZ instrument onboard a long-duration balloon into a photochemical model to intercompare measurements taken with the same instrument at different times. They generally find a good agreement and conclude that the night-time chemistry of NO$_y$ is generally well understood. To our knowledge, photochemistry models have not been used so far to validate NO$_2$ satellite measurements made at different SZAs. However, there is a study by Marchand et al. (2004) that assimilates NO$_2$ and O$_3$ measured by GOMOS into a model to investigate the self-consistency of GOMOS night-time NO$_2$, O$_3$ and NO$_3$ measurements.

In this study a 1-dimensional photochemical model was used in order to transform the NO$_2$ measurement from solar occultation to the SZA during the SCIAMACHY NO$_2$ measurement. We provide a detailed description on the method used for transforming the solar occultation measurements to the selected SZA of the limb measurements of SCIAMACHY. A sensitivity study is presented and used in assessing the comparison of the NO$_2$ profiles retrieved from the different satellite sensors. The first results of the comparisons between SCIAMACHY and HALOE, and SCIAMACHY and SAGE II from summer/fall 2002 are shown.

2 Satellite NO$_2$ data sets and collocation criteria

2.1 SCIAMACHY-IUP stratospheric NO$_2$ profiles V1

SCIAMACHY on the recently launched satellite ENVISAT is a passive remote sensing instruments, which measures the back scattered reflected and transmitted electromagnetic radiation up welling from the atmosphere in different viewing geometries. SCIAMACHY comprises eight spectral channels between 240 and 2380 nm with a channel dependent spectral resolution of between 0.2 and 1.5 nm. SCIAMACHY is the first satellite instrument, which makes spectroscopic observation of the upwelling radiation at the top of the Earth's atmosphere in nadir viewing and limb viewing geometries, as well as the solar and lunar occultation modes. For this study only data from SCIAMACHY limb observa-

tions have been used. These yield NO$_2$ profiles having almost global coverage (within six days) and a reasonably high vertical resolution. In the novel limb scattering method, the line of sight follows a tangential path through the atmosphere and solar radiation is detected that is scattered along the line of sight into SCIAMACHY's field of view, and transmitted from the scattering point to the instrument. SCIAMACHY scans the tangent height (TH) range between about -3 and 100 km with TH steps of about 3.3 km. SCIAMACHY limb measurements are performed during the day and cover the SZAs between around 20° and 92°. Further information on the SCIAMACHY instrument and its mission objectives are provided in Bovensmann et al. (1999).

For this study, the NO$_2$ profiles have been retrieved from the SCIAMACHY level 0 data, which are radiometrically and spectrally uncalibrated signals. The signal counts have been integrated over the entire azimuth scan of 960 km, which yields the optimal signal-to-noise ratio. At a later date retrievals at the four different azimuth angles, measured at each tangent height by SCIAMACHY are planned. The data are divided by the integration times and a dark current correction is performed by substracting the spectrum at 150 km tangent height. SCIAMACHY NO$_2$ profiles, called SCIAMACHY-IUP NO$_2$ profiles V1, are derived from the retrieval method described in detail in Eichmann et al. (2004) and von Savigny et al. (2004). The retrieval is performed in the spectral range 420–455 nm using ratios of limb spectra in a selected tangent height region to a limb measurement at a reference tangent height of around 40 km.

The measurements of the scattered solar radiation in limb viewing geometry as performed by the SCIAMACHY instrument are simulated using the CDI radiative transfer model (Rozanov et al., 2001). This model calculates the limb radiance by accounting for the single scattered radiance properly and using an adequate approximation to determine the multiple scattering. The optimal estimation method is used for the retrieval of the Stratospheric NO$_2$ profiles for the altitude range from about 15 up to 35–40 km. The accuracy in retrieved number densities is estimated to be about 15–20% between 15 and 30 km. Outside this altitude range, and for meteorological situations with little or no stratospheric NO$_2$ larger errors are expected.

2.2 Satellite occultation data used for comparisons of satellite NO$_2$ profiles

Both instruments used to validate SCIAMACHY NO$_2$ data, HALOE and SAGE II, measure trace gas profiles during fifteen spacecraft sunrises and sunsets daily, normally in opposite hemispheres, although at certain times of the year these measurements occur on the same day and almost overlap in space. Both solar occultation modes correspond to a good approximation to a SZA of 90°. The latitudes of the NO$_2$ profiles, observed by HALOE and SAGE II, change from one

day to the next such that sampling of the global atmosphere between about 70° S and 70° N results over a 1-year-period.

2.2.1   HALOE NO$_2$ measurements

The HALOE instrument was launched in September 1991 on board the Upper Atmosphere Research Satellite (UARS) and routine observations by HALOE started in October 1991. In this study we made comparisons to Version19 (v19) of the HALOE NO$_2$ data product. After an extensive validation of v17 by Gordley et al. (1996), the quality of Version 18, v18, HALOE NO$_2$ data is characterized on the HALOE web page (http://haloedata.larc.nasa.gov). V18 data agree with correlative observations from 25 to 45 km within the ±10 to ±15% level, with no obvious bias. The NO$_2$ data are described as excellent from the tropopause to 25 km in clear air conditions, but exhibit a low bias in the presence of aerosols. The aerosol correction in the lower stratosphere below about 20 km is large being more than 100%. However, the data from the last 5 years should be more accurate because the aerosol loading is at its lowest since 1978, because of the lack of volcanic intrusions into the stratosphere. Randall et al. (2002) compared HALOE v19 NO$_2$ data to data from Atmospheric Trace Molecule Spectroscopy Experiment (AT-MOS). Results show that between 25 and 42 km the measurements from the two instruments agree within 10%. ATMOS NO$_2$ data have an estimated accuracy of about 6% in the 20 to 45 km range (Abrams et al., 1996). The vertical resolution of HALOE NO$_2$ data is given with 2 km (Gordley et al., 1996).

2.2.2   SAGE II NO$_2$ measurements

The longest record of satellite high-resolution NO$_2$ profile measurements have been made by the solar occultation instrument SAGE II which was launched on the Earth Radiation Budget Satellite (ERBS) in October 1984 and is still operational. The instrument field of view in the direction normal to the line of sight is 0.5 km vertically by 2.5 km horizontally. The NO$_2$ measurements are derived from the difference between the absorptions in narrow bandwidth channels centered at 448 and 453 nm. The vertical resolution of SAGE II NO$_2$ data is around 2 km. In the extensive SAGE II NO$_2$ validation study on a much older data version by Cunnold et al. (1991), the precision of the profiles is about 5% and the absolute accuracy of the measurements is estimated for sunset measurements to be 15%, based on uncertainties in the absorption cross-section and their temperature dependence. Agreement of approximately 10% was seen in comparisons to balloon-measured profiles over Southern France between 23 and 32 km altitude (the highest altitude of the balloon observations) and to ATMOS profiles obtained four days later between 23 and 37 km altitude. The SAGE II data version 6.1, the forerunner of the version used in this study, is characterized to have achieved a significant improvement in

the NO$_2$ retrievals through a minor modification to the spectroscopy, which cause a concomitant improvement to short wavelength aerosol extinction particularly in the lower stratosphere and during low aerosol loading periods (SAGE II website: http://www-sage2.larc.nasa.gov/data/v6_data/). As stated by Larry Thomason (PI of SAGE II project, pers. com., 2004), SAGE II NO$_2$ data version 6.1 and 6.2 are considerably better than version 6.0, but still biased by about 10% compared to HALOE.

2.3   Data sets

All available SCIAMACHY-IUP NO$_2$ profiles V1, HALOE v19, and SAGE II v6.2 data sets from 24 July 2002, and for the period from 12 September 2002 to 14 October 2002 were searched for near coincident measurements. The time period for the comparison was chosen because for the time around the split of the Antarctic ozone hole at 27 September 2002 more SCIAMACHY level-0 data were available than during other times.

2.4   Spatial and time distance criteria for coincident measurements

SCIAMACHY NO$_2$ profiles have been compared with HALOE and SAGE II measurements for the coincidence criteria that measurements took place on the same day and that the tangent point of HALOE or SAGE II is within 500 km of the centre of the nearest SCIAMACHY ground pixel. This ensures that the HALOE or SAGE II tangent point is within or near the SCIAMACHY ground scene which is rather large for SCIAMACHY being about 960 km×400 km.

2.5   Criteria for coincidences within the same air mass

Validation at the edge of different air masses is more difficult, because gradients in the horizontal distribution result from transport processes, e.g. at the polar vortex or at the upper troposphere lower stratosphere region (UTLS). Therefore, besides to identifying collocated measurements by limiting time difference and distance between two observation points, additional criteria were selected to ensure that collocations were made in the same air masses according to the method described in Bracher et al. (2004). The tropopause height and the position of the polar vortex were determined by analysis of the potential vorticity (PV) distribution. PV values measured at the same geolocation and day of each collocated measurement were taken from the United Kingdom Meteorological Office (UKMO) assimilated meteorological dataset available in a 3.75°×2.5° (longitude-latitude) grid resolution (Swinbank and O'Neill, 1994) and spatially interpolated to the observation point. As a result of the relatively large ground scene of a SCIAMACHY profile, the corner coordinates of the ground scene for each SCIA-MACHY profile were checked for their homogeneity of PV. For samples outside the tropics, the tropopause was assumed

to be the 3.5 PVU level, which was shown by Hoerling et al. (1991) to be a good estimate for the dynamical tropopause height. Inside the tropics where the dynamical tropopause is not defined, the 380 K isentropic level was a proxy for the tropopause. To separate collocations, where the four corners of a SCIAMACHY ground pixel and the collocated HALOE or SAGE II tangent point were inside the polar vortex or outside the vortex, matches where the PV of both measurements at the isentropic level of 475 K were selected having either greater than 40 or less than −40 PVU (i.e. inside the vortex) or between −30 and 30 PVU (i.e. outside the vortex), respectively. For the tropopause height, deviations within 1 km for collocations were tolerated.

This applied method is fast in screening a larger number of collocations for their coincidence regarding air masses. Bracher et al. (2004) showed that including these atmospheric dynamics criteria concerning tropopause height and polar vortex for the selection of collocated measurements improves significantly individual comparisons. Opposed to that, for comparisons of multi-platform measurements where only a small amount of matches have been found within a chosen spatial-temporal vicinity the methods developed by Bacmeister et al. (1999), Lu et al. (2000), and Danilin et al. (2002) to enlarge the number of matching by using a trajectory hunting technique is more appropriate. The results of these studies showed that in this case with the trajectory hunting technique comparisons were statistically more robust than just limiting the comparisons to the traditional correlative analysis.

3   Model used for scaling NO$_2$ measurements

As pointed out above, NO$_2$ in the stratosphere is relatively short-lived, and has a significant diurnal variability. The livecycle of NO$_2$ is determined by a fast exchange between NO and NO$_2$ (R7 and R8), and the slow formation of N$_2$O$_5$ (R4 and R5). During the night, N$_2$O$_5$ is in thermal equilibrium with NO$_2$ and NO$_3$, and also reacts on liquid surfaces to form HNO$_3$. During the day, the partitioning between NO, NO$_2$ and N$_2$O$_5$ depends strongly on SZA due to the rapid photolysis of NO$_2$ and the slower photolysis of N$_2$O$_5$. This dependency on SZA makes validation of NO$_2$ measurements difficult, as measurements seldom coincide both in location and local time. In order to compare collocated solar occultation NO$_2$ measurements at 90° SZA to NO$_2$ measurements from SCIAMACHY at various SZAs, a one-dimensional chemical and photolysis model of the stratosphere that extends from the tropopause up to the stratopause has been used.

The model chemistry is similar to the SLIMCAT chemistry scheme. Reaction rates and absorption cross sections are taken from the JPL 2000 recommendation (Sander et al., 2000). The height of the model boxes can be adapted to fit the altitude resolution and tangent altitudes of either the occultation or SCIAMACHY measurement. The model includes 135 chemical reactions including gas-phase as well as heterogeneous reactions, and 44 photolysis reactions of the 52 species most important for stratospheric chemistry, and runs with a chemical time-step of 5 min. Model output is every 15 min.

The one-dimensional model has been used to compare satellite measurements of NO$_2$ at different SZAs in the following way. The model is initialised with the output of a global 2-D chemistry, transport and photochemistry model for the geolocation and day of the measurement. The 2-D model is a composite of the SLIMCAT chemistry scheme (Chipperfield, 1999) and the THIN AIR dynamics code (Kinnersley, 1996), and is described in more detail in (Sinnhuber et al., 2003). The chemistry scheme of the one-dimensional model is derived from the chemistry scheme of the 2-D model, and considers exactly the same photochemical reactions and species. The only difference is that the onedimensional model does not use simplifications of the behaviour of very short-lived species assuming photochemical equilibrium. O$_3$ is initialised based on measurements whenever available. The model is run over a period of 3 days to allow for spin-up, and on the third day, NO$_2$ at sunset or sunrise from the model is compared to the occultation measurement. Then, the NO$_x$ species – NO, NO$_2$ and N$_2$O$_5$ – from the model are scaled to fit the validation measurement's NO$_2$ at sunset or sunrise. The model is run again for three days with the modified NO$_x$.

The model result and SCIAMACHY measurement are compared at the SZA of the SCIAMACHY measurement. In the ideal case of two perfect instruments and a perfect photochemical model, model and measurement would agree. In reality, not only do the measurements suffer from instrument noise and systematic measurement errors, but also the model is imperfect and has its own additional errors. The uncertainty on the ability of the model to account for the variation of NO$_2$ as a function of SZA needs to be assessed.

3.1   Sensitivity Study with the photochemical model

O$_3$ plays a major role in the NO$_x$ partitioning, because O$_3$ reacts with NO and NO$_2$, and also impacts photolysis as a result of its strong UV absorption. Other parameters that influence the outcome of the comparison are temperature, which is important because of the temperature dependency of the reaction and photolysis rates, and also for the thermal decomposition of N$_2$O$_5$; the aerosol loading of the atmosphere, represented by the amount of H$_2$SO$_4$, is important for the hydrolysis of N$_2$O$_5$. Another factor that influences the outcome of the comparison is the variation of the SZA of the validation measurement along the instruments line-of-sight. By definition, the SZA of the occultation measurement is 90° at the tangent point, however, before the tangent point, the SZA is larger, after the tangent point, it is smaller than 90°. As the variability of NO$_2$ is largest during sunset and sunrise, this affects the initialisation of NO$_x$ in the model.

The most obvious source of model uncertainties are inaccuracies in the knowledge of the photolysis frequencies for the photochemical reactions and the reaction rate coefficients used in the model. All reactions that are known to play a major role for stratospheric chemistry are included. The reaction rates, taken from the JPL 2000 recommendation, are based on measurements that themselves have measurement errors. The profiles of NO_2 and O_3 for the model are initialised using the occultation measurement as described.

Sensitivity studies were carried out to investigate the impact of the model uncertainty on the measurement comparison exemplarily for one SCIAMACHY measurement of 23 August 2003 at 54.2° S. This is compared to a SAGE II sunset measurement of the same day at approximately the same location. For the sensitivity studies, model runs were carried out varying the parameters in question over a reasonable range, and comparing the model result to the model "base" run where all parameters have their "default" setting. Model altitudes are scaled to the SAGE NO_2 measurement, and extend from 15.5 km to 42 km for this model run. The comparison with the base run is carried out for the SZA of the SCIAMACHY measurement, 76.12°, as well as for 120° for a night-time scenario. This later case is also of interest for example for the validation of MIPAS and GOMOS, which measure during nighttime. As the dominating processes during the night are not the same as during daytime, results could be very different. The relative differences between "base" and each test model run are plotted in Fig. 1 for the day and night scenario, respectively.

3.1.1 Ozone

The default model run is initialised with an O_3 measurement of the SAGE instrument that was taken simultaneously with NO_2. To take into account O_3 absorption above the altitude range of the model, an O_3 density of $7e16\,cm^{-2}$ is initialised above the model range, derived from the SAGE O_3 measurement between 42 and 58 km. In one set of model runs, the O_3 is scaled by a factor of 1.5. This is a rather conservative estimate for dynamic O_3 variability. It leads to about 5% larger NO_2 values below 30 km during daytime, and to about 13% smaller NO_2 values during night-time (Fig. 1). In another set of model runs, the O_3 column above the model altitudes is set to zero. This affects the NO_2 amount mainly above 35 km; there, differences to the "base" run including the O_3 column are rather large: being up to 20%. During the day, reducing the O_3 column above the model altitudes leads to a decrease of NO_2, whereas during the night, modelled NO_2 increases.

3.1.2 Temperature

In the default setting, temperature is initialised by the 2-D model output which calculates temperature itself. Temperature measurements would be preferable of course, but are not always available. For the sensitivity studies, temperature

was varied by 10 K compared to the "base" run. This appears a reasonable estimate for the deviations from a temperature climatology – the 2-D model output – to the true temperature, which is unknown. A 10 K increase in temperature decreases NO_2 slightly between about 35 and 25 km, and increases NO_2 above and below (see Fig. 1). Again, during night-time, the differences to the "base" run are much larger than during day, reaching a 12% decrease between 20 and 25 km. During day-time, differences are much smaller, with maximal differences of about 5% reached at about 40 km altitude. This is due to the fact that during the night, the thermal equilibrium between N_2O_5 and NO_2 plays a larger role.

3.1.3 Aerosol loading

The aerosol loading of the atmosphere determines the partitioning between NO_x – NO, NO_2, and N_2O_5 – and HNO_3 through the hydrolysis of N_2O_5. As NO_x is fixed in the model run, the aerosol loading should not play a large role in determining NO_2. Two factors were varied to test this hypothesis: the amount of H_2SO_4, and the reaction rate of N_2O_5 hydrolysis on liquid aerosols. The amount of H_2SO_4 was decreased and increased by a factor of 10. Decreasing H_2SO_4 has no significant impact on NO_2, while increasing H_2SO_4 increases NO_2 slightly below 25 km during daytime; during nighttime, NO_2 is hardly affected (see Fig. 1). The gamma coefficient of N_2O_5 uptake on liquid aerosols is varied by the maximum and minimum values, given in the JPL recommendations, 0.05 and 0.2 (the default value in the model is 0.1). Again, decreasing gamma does not change NO_2 significantly, while increasing gamma leads to slightly higher values below 25 km during daytime (Fig. 1). The fact that NO_2 seems rather insensitive to the aerosol reactions is probably due to the fact that the aerosol loading of the 2-D model is low, initialised by SAGE measurements from the year 1995. This is realistic for the current post-Pinatubo area, but the situation would be different in situations with higher aerosol loading, i.e. shortly after a large volcanic eruption depositing significant amounts of aerosol in the stratosphere.

3.1.4 Reactions important for NO_x partitioning

The impact of uncertainities in the reaction rates of the two reactions most important for the partitioning between NO and NO_2, photolysis of NO_2, (R7) and reaction of NO with O_3, (R8) were investigated within the sensitivity study. For the NO_2 absorption cross section, an error of 5–10% is given in the JPL recommendation, while it is stated that "the agreement is poor below room temperature", i.e. at stratospheric temperatures (DeMore et al., 1997). To reflect this, the NO_2 photolysis rate was decreased by 20%. This leads to an increase in NO_2 of less than 5% between 35 and 25 km increasing to 12% below 20 km during the day. NO_2 levels during the night are strongly affected as well, decreasing by about 10% over the whole altitude range (Fig. 1). For reaction (R8),
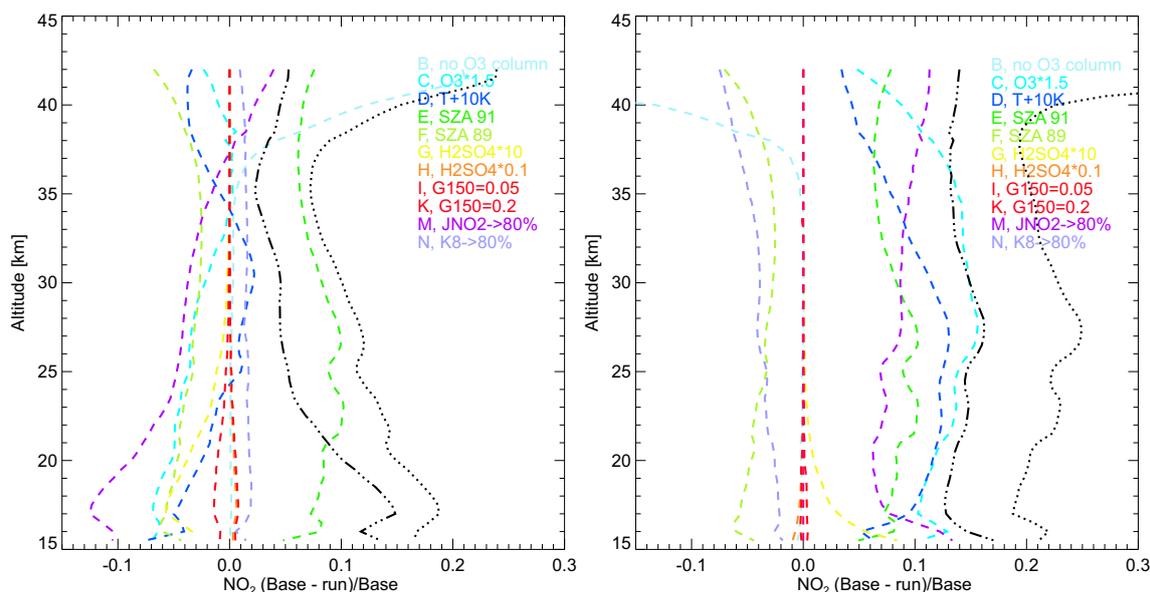
Fig. 1. Relative difference of "base" model run to the test model runs for a solar zenith angle (SZA) of 76,1° corresponding to the SCIA-MACHY measurement (left), and for a SZA of 120° (right). Black dashed line: total statistical uncertainty, black dash-dotted line: total uncertainity without the contribution of O$_3$ (B and C) and sza (E and F). The calculation of the individual uncertainity contributions and the total uncertainity are described in Sect. 3.1.

no errors are given; for the sensitivity study, again an uncertainty of 20% is assumed, and the reaction rate of (R8) was decreased by 20%. This decreased NO$_2$ by about 2% during the day, and increased NO$_2$ by 2 to 8% during the night (Fig. 1).

3.1.5 Solar zenith angle variations along line-of-sight

The SZA of an occultation measurement is 90° at the tangent altitude. However, the SZA varies along the line-of-sight (LOS) of the instrument thus that it is larger before and smaller behind the tangent altitude. This means that the measurement of an occultation instrument is a superposition of different SZAs near 90°. As NO$_2$ is highly variable during sunset and sunrise, even a small uncertainty in the SZA of the occultation measurement can lead to large errors in the initialisation of the model NO$_x$. A simple geometric consideration shows that along the LOS, already one kilometer away from the tangent point the SZA has changed by nearly 1°, positive before, and negative after the tangent point. If NO$_2$ changed linearly with the SZA, these changes would cancel each other out. However, this is not the case, and the variation of the SZA along the LOS of an occultation instrument does influence the retrieved density especially below 20 km (Newchurch et al., 1996). It is possible to correct for this variation during the NO$_2$ retrieval as it is done for the HALOE retrieval (see Gordley et al., 1996), but this carries its own sources of additional errors, and is not done for all occultation measurements (Randall et al., 2002). For the sensitivity study, the SZA of the validation measurement is varied

by 1°. This leads to differences in modelled NO$_2$ of up to 10% (Fig. 1). This is probably a rather conservative estimate of the possible model uncertainty arising from the variation of the solar zenith angle along the line-of-sight of the occultation measurement, but still this is one of the largest source of model uncertainties. Variations along the LOS of the ENVISAT limb measurement do not play a similar large role, as the variability of NO$_2$ is by far larger during sunrise and sunset.

3.1.6 Model drift

Every model drifts, meaning that trace gas concentrations differ slightly from day to day even if all other parameters – temperature, pressure, SZA variations – are completely the same. One reason for this is numerical drift, but the more important fact is that the atmosphere itself is not an equilibrium system. Model drift can not be avoided, but has to be considered for the overall model uncertainty. Here, model drift for NO$_2$ is determined by comparing to the occultation measurement: NO$_2$ in the model is initialised to agree with the occultation measurement during sunrise or sunset. If there was no model drift, after three days of model run, model NO$_2$ during sunrise or sunset would therefore agree perfectly with the occultation measurement. In fact, between 25 and 40 km, they agree within 2%, but above and below, the model drift of NO$_2$ can reach up to 10% (Fig. 2).
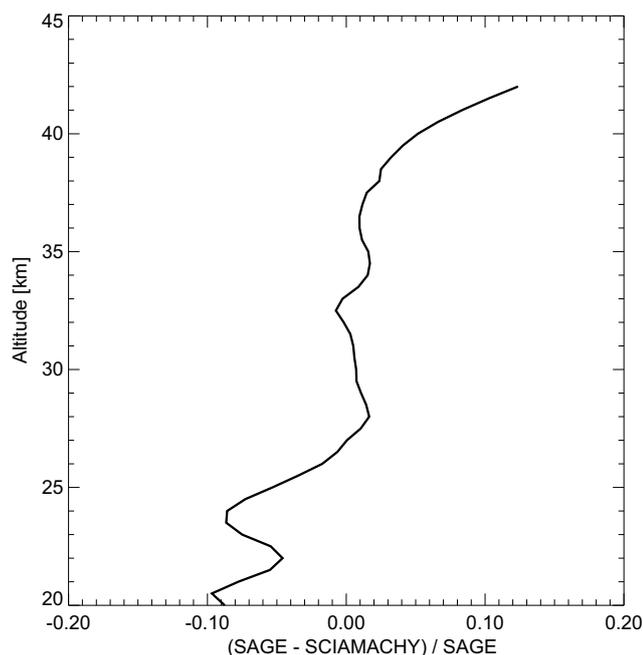
Fig. 2. Relative difference of model at 90° to the SAGE measurement, as an indicator of the model drift.

3.1.7   Total model uncertainty

From the different uncertainty sources considered in the sensitivity studies, a total uncertainty of the model calculation is estimated. As the different uncertainties are not correlated, the uncertainty is calculated statistically, as the root mean square of the individual uncertainty contributions. The total uncertainty is also shown in Fig. 1 (black dotted line). During the day, it reaches maximum values of 19% below 20 km, decreasing to about 8% between 35 and 40 km. Above 40 km, it rises sharply to values larger than 20%. The largest contributions to the overall uncertainty during the day are the SZA variations of the occultation measurement, the NO$_2$ photolysis rate, and the O$_3$ profile; above 40 km, the O$_3$ column density above the model top altitude dominates, while below 20 km, H$_2$SO$_4$ plays a role as well. During the night, the overall uncertainty is about 20% between 15 and 40 km, rising sharply to over 30% above 40 km. During the night, the uncertainty again is dominated by the O$_3$ profile, and the SZA variation of the occultation measurement and NO$_2$ photolysis play a large role as well. NO$_2$ photolysis is probably important as it defines NO$_2$ during sunset, at the beginning of the night. But the second largest uncertainty source during the night is temperature, and the reaction of NO and O$_3$ plays a role as well. The overall uncertainty is nearly double as large than during the day in the 20 to 40 km range, mainly because the contributions of O$_3$ and temperature are so much larger. It concludes that, as the additional model uncertainty is so much larger, validation of night-time measurements with occultation measurements are more dif-
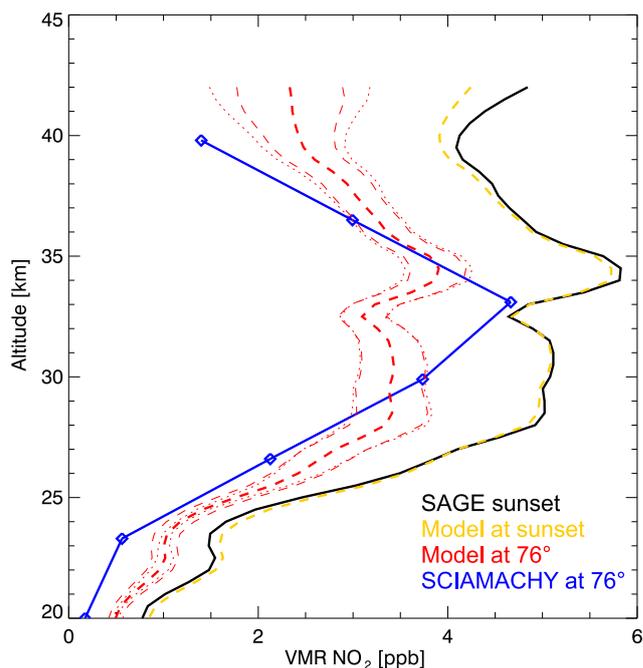
Fig. 3. Comparison of SAGE (black) and SCIAMACHY (blue) measurements of 23 August 2003 at 54.2° S, and model results for the same day and at SAGE and SCIAMACHY solar zenith angles (red and yellow). Red dotted line describes the total uncertainty of the model, red dashed line the total uncertainty including model drift.

ficult than validation of day-time measurements. However, two of the larger uncertainty sources, due to O$_3$ and due to temperature, can be avoided by using measurements for the initialisation of the model. Variations in O$_3$ result in similarly large uncertainties, but those were easily avoided in our validation as simultaneous retrievals of O$_3$ were readily available from HALOE and SAGE II, but are also available for SCIAMACHY and the two other atmospheric ENVISAT instruments, MIPAS and GOMOS. Taking O$_3$ from the occultation measurement and correcting for the variability of the SZA along the LOS of the occultation measurement as it has been done for the validation of SCIAMACHY profiles with HALOE decreases the model uncertainty to less than 5% between 20 and 40 km during the day, and to about 14% during the night (see Fig. 1, dash-dotted black line).

Finally, the comparison of the SAGE and SCIAMACHY measurements of 23 August 2002 is shown in Fig. 3. Also shown are the model results for sunset and the SZA of the SCIAMACHY measurement, as well as the total model uncertainty. The model uncertainty due to model drift is shown separately; it appears that it plays a role only above 40 km. While the agreement between the SCIAMACHY measurement and the model result at the SCIAMACHY SZA is much better than the agreement between SCIAMACHY and SAGE, the overall agreement is still not very good in
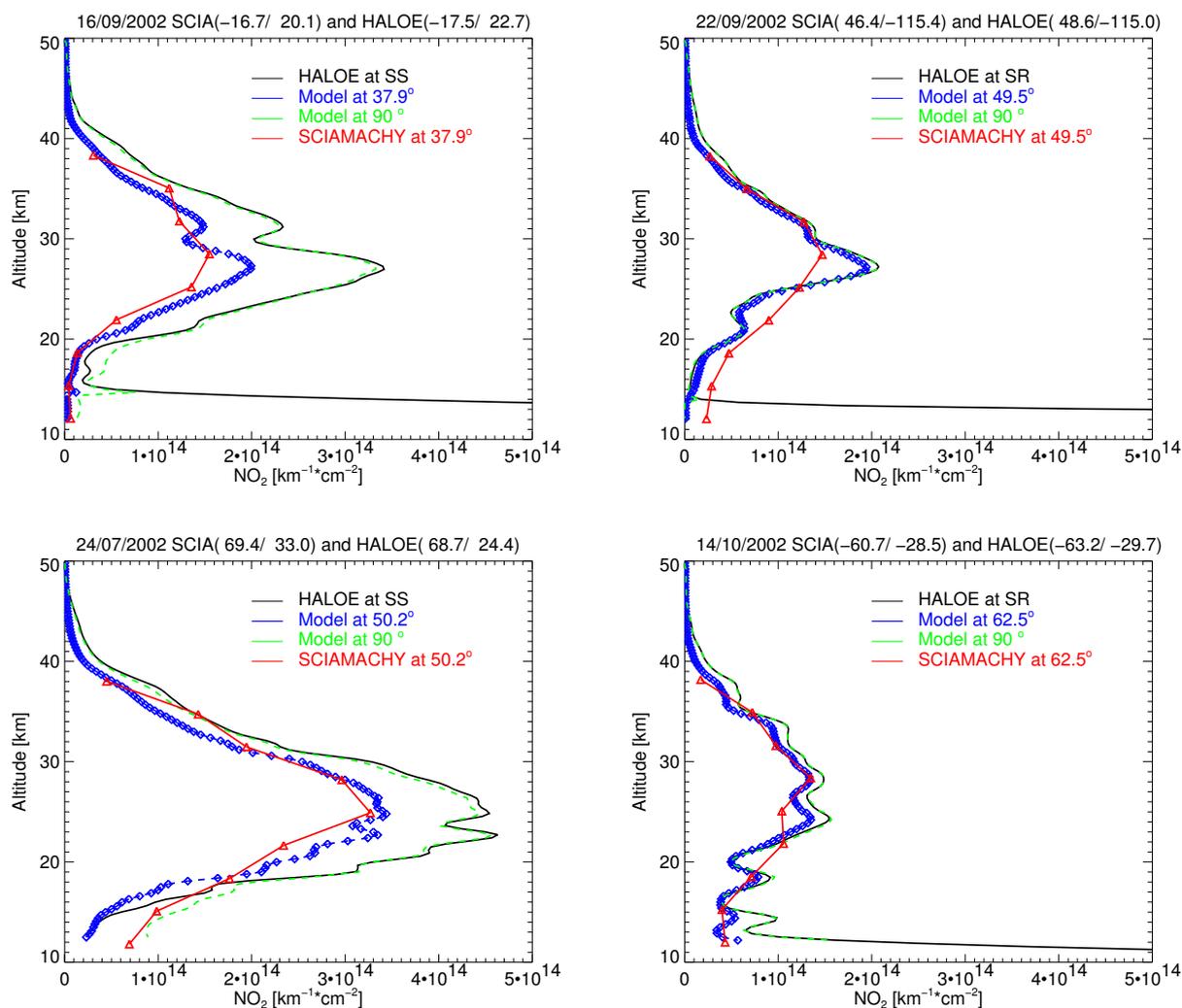
Fig. 4. Comparisons of NO$_2$ profiles from collocated HALOE (black) and SCIAMACHY (red) measurements with results from model runs described in Sect. 3: the model at 90° (green) signifies where the model was scaled in such a way that NO$_2$ values correspond to the HALOE NO$_2$ measurement at the HALOE SZA of 90° in dependence when the measurement was taken (during sunrise or sunset). Taking the model at 90° NO$_2$ values and running them to the certain solar zenith of the SCIAMACHY measurement, gives the modelled NO$_2$ profile at SCIAMACHY solar zenith angle (model at SCIAMACHY SZA in blue). Examples from: the tropics at ∼38° SCIAMACHY SZA and HALOE sunset (SS) measurement at 16 September 2002 (top left), from the mid latitudes at ∼50° SCIAMACHY SZA and HALOE sunrise (SR) measurement at 22 September 2002 (top right), from the high northern latitudes at ∼50° SCIAMACHY SZA and HALOE SS measurement at 24 September 2002 (bottom left), and from the high southern latitudes at 62.5° SCIAMACHY SZA and HALOE SR measurement at 14 September 2002 (bottom right).

this case: below 28 km and above 37 km, SCIAMACHY is significantly lower than the modified SAGE measurement, while at 33 km, SCIAMACHY is significantly higher than the modified SAGE.

4 Validation of SCIAMACHY NO$_2$ profiles

Overall, 52 collocated SCIAMACHY-IUP and HALOE, and 60 collocated SCIAMACHY-IUP and SAGE II NO$_2$ measurements have been identified. These collocated measure-

ments were investigated in two sets, determined by the SCIA-MACHY level 0 data availability:

i) 24 July 2002, and,

ii) from 12 September 2002 to 14 October 2002.

While the matches between SCIAMACHY and HALOE were distributed globally, the majority of collocations were at high and mid latitudes between 45° to 69°: 31 in the northern and 9 in the southern hemisphere. The matches between SCIAMACHY and SAGE II were all in high latitudes above

Table 1. Statistical results of the comparison of SCIAMACHY NO$_2$ profiles at a certain solar zenith angle (SZA) to HALOE NO$_2$ profiles measured during sunset (SS) or sunrise (SR) and scaled with the in Sect. 3 described model to the SCIAMACHY SZA. Statistical results are given for different SCIAMACHY SZA ranges and only matches within the same air mass are included: number of collocations within the SZA range (N), latitudinal range (latitude), HALOE occultation type (type), mean relative deviation (MRD), the altitude range for which MRD is given (altitude) and the root mean square of the MRD at these altitudes (RMSRD).

SZA range	N	latitude	MRD	altitude	RMSRD	type
30° to 40°	3	tropics and subtropics	−7% to 20%	22 to 34 km	10%–30%	2 SS, 1SR
40° to 50°	5	5 at 40° N–68° N	−8% to 15%	20 to 33 km	10%–30%	2 SS, 3 SR
50° to 60°	8	5 at 40°–50° N, 3 at 40°–60° S	−15% to 10%	20 to 33 km	8%–35%	5 SS, 3 SR
60° to 70°	21	15 at >55° N, 6 at >60° S	−10% to 12%	22 to 33 km	15%–25%	5 SS, 16 SR
all matches	37	from 69° N to 66° S	−7% to 12%	21 to 33 km	10%–30%	14 SS, 23 SR

60°: 36 in the northern and 24 in the southern hemisphere. The NO$_2$ satellite validation was chosen to lie within the time of the ozone hole. In this particular year, a major warming event occurred over the Antarctic region, probably the first ever recorded in the southern hemisphere (e.g. Weber et al., 2003). It was therefore essential for the validation to identify homogeneous air masses.

For the SCIAMACHY and HALOE comparison and after applying the criteria of homogeneity explained in Sect. 2.5, 37 data sets remained. For the excluded matches, for twelve cases, the tropopause height varied strongly within the SCIAMACHY scene, compared to that of the HALOE measurement. In three cases matches from high southern latitudes were excluded because the measurements were taken across the edge of the polar vortex. Only one match was found where both measurements were completely within the polar vortex (see Fig. 4 bottom right). Table 1 shows the distributions of the SCIAMACHY and HALOE collocations in different latitudinal zones, ranges of SCIAMACHY SZAs and type of HALOE measurement. The majority of matches are in the high northern latitudes and at SCIAMACHY SZA above 60°, and HALOE NO$_2$ values above 60° latitude were determined from sunrise solar occultations. For the SCIAMACHY and SAGE II comparison, only 25 collocation pairs of measurements were identified as being from the same air mass. All matches from the high southern latitudes lie in areas of highly variable PV across the edge of the polar vortex. From the Northern hemisphere, 11 matches were excluded because of large differences in the tropopause height. The 25 matches included in the NO$_2$ comparison were all measured between the 12 September 2002 and the 9 October, 2002.

4.1 Examples of NO$_2$ profile comparisons from satellite data

Figure 4 presents four examples of the comparison of HALOE and SCIAMACHY NO$_2$ profiles from different latitudes (tropics, mid and high latitudes) and at different SCIAMACHY SZA (around 40°, 50°, 60°). Also shown are results of model calculations, which account for the difference

in SZA of the two instruments and therefore the NO$_2$ profile. This is achieved by converting the HALOE profiles to that expected for of the SCIAMACHY SZAs. The method uses a photochemical model initiated with the HALOE profile, as described in Sect. 3. Two types of modelled NO$_2$ profiles are shown. The "model at 90°" indicates where the model NO$_x$ was scaled in such a way that NO$_2$ values correspond to the HALOE NO$_2$ measurement, during sunset or sunrise. Comparing the model results at 90° to the HALOE (or SAGE II) measurement illustrates the potential of the model to be applied for scaling NO$_x$ to make measurements taken at different SZAs, comparable.

In all comparisons, the NO$_2$ value from the model at 90° and the HALOE (seen in Fig. 4) or SAGE II (results not shown) measurement corresponded well above 20 km. Overall, above 20 km the SCIAMACHY NO$_2$ values agree well with the HALOE measurement scaled to the SCIAMACHY SZA. Below 20 km the SCIAMACHY NO$_2$ values are much larger than the HALOE measurement scaled to SCIAMACHY SZA for two examples shown (Fig. 4, top right and bottom left), while at the comparison within the polar vortex (Fig. 4, bottom right) and the tropics (Fig. 4, top left) the SCIAMACHY and the scaled HALOE measurement agree well even down to 12 km. Due to the coarser vertical resolution of SCIAMACHY, detailed structures like the double peak in the example in the tropics (Fig. 4, top left) are not resolved, and in the example from the mid-latitudes at around 50° SZA (Fig. 4, top right) this leads to an underestimation of the NO$_2$ maximum.

Figure 5 shows four examples of the comparison of SAGE II and SCIAMACHY NO$_2$ profiles in the high northern latitudes at mid September where also collocations of SCIAMACHY with HALOE had been identified. Model values for the SCIAMACHY SZA with the input of the HALOE or SAGE NO$_2$ values are given in addition to the SCIAMACHY, SAGE and HALOE NO$_2$ measurements. The SCIAMACHY SZA of the example shown here varies from 65° to 67.5°. Since HALOE measurements were taken during sunrise and SAGE II measurements during sunset, these
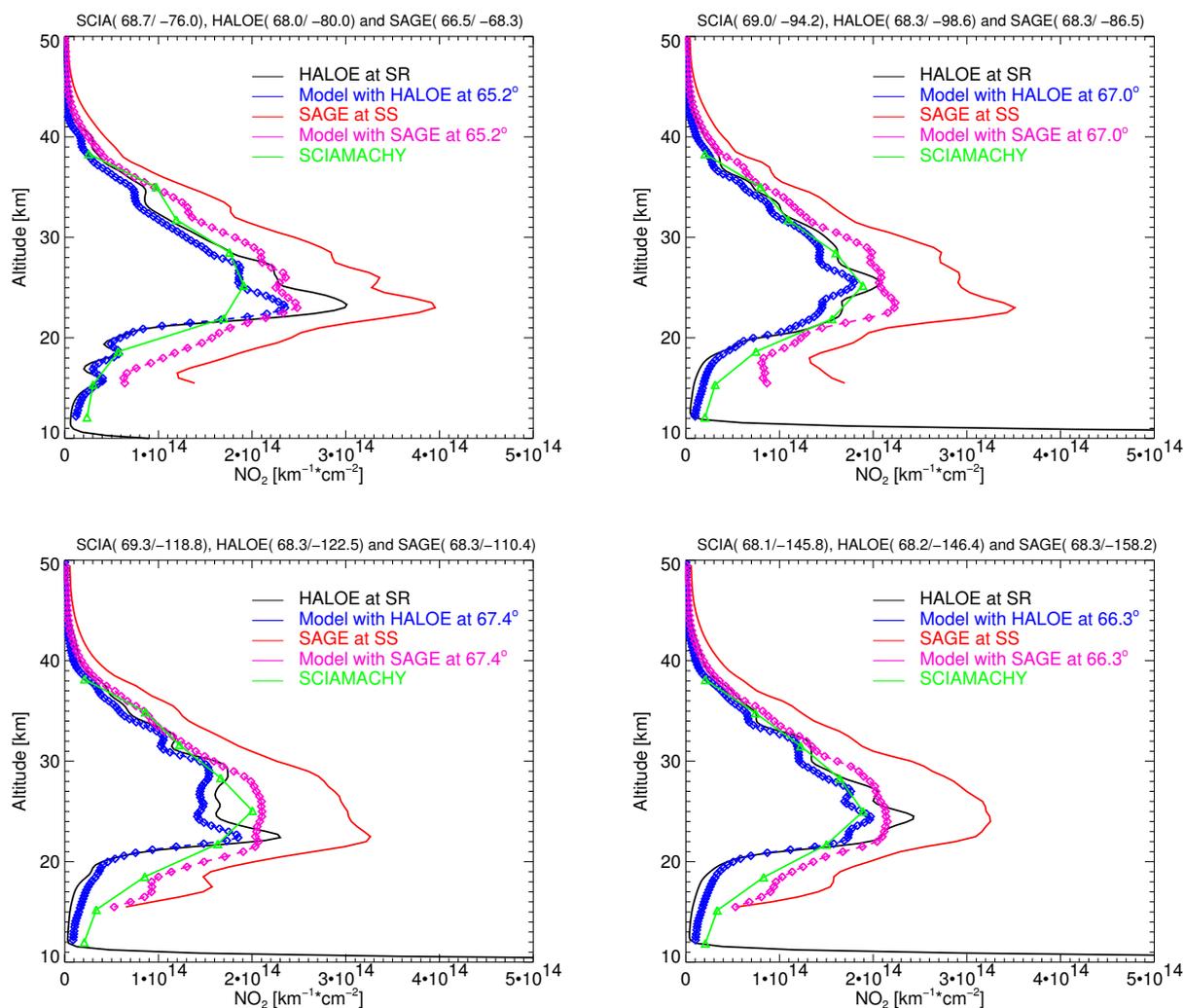
Fig. 5. Comparisons of NO$_2$ profiles from collocated HALOE (black), SAGE (red) and SCIAMACHY (green) measurements with results from model runs described in Sect. 3. All HALOE measurements were taken during sunrise (SR) and all SAGE measurements during sunset (SS). The model with HALOE at SCIAMACHY SZA (blue) signifies where the model was scaled in such a way that NO$_2$ values correspond to the HALOE measurement at the HALOE SZA of 90° during sunrise and then scaled to the SZA of the SCIAMACHY measurement by using a 1-dim model. In accordance to that, the model with SAGE at SCIAMACHY SZA (pink) was determined using the SAGE NO$_2$ measurement as an input for the model value at SAGE SZA of 90° during sunset and scaling this model value by using a 1-dim model scaled to the SZA of the SCIAMACHY measurement. Examples are either from 12 (top left) or from 16 September 2002 (other three examples).

measurements cannot be directly compared, but rather the scaled values determined by combining the data products with the photochemical model are compared. In all examples, SAGE II NO$_2$ values scaled to the SCIAMACHY SZA are significantly higher than NO$_2$ profiles of SCIAMACHY, and also higher than HALOE measurements scaled to SCIAMACHY SZA. SCIAMACHY NO$_2$ profiles show good agreement with the scaled HALOE profiles above 20 km. Despite the coarser vertical resolution of SCIAMACHY in two comparisons (Fig. 5, top and bottom left), the SCIAMACHY retrieval resolves the profile structure,

which is comparable to that in the scaled HALOE profile. However, the SCIAMACHY NO$_2$ maximum in one comparison is lower than that of the scaled HALOE profile (Fig. 5, top left). In Fig. 5 (bottom left) SCIAMACHY measured higher values at the peak than HALOE data, being closer to the scaled SAGE II values and reflecting the SAGE II scaled profile structure. Below 20 km, SCIAMACHY NO$_2$ values are close to scaled HALOE values in one comparison (Fig. 5, top left), and close to the scaled SAGE II NO$_2$ values in two comparisons (Fig. 5, bottom left and right), and in between the two in one comparison (Fig. 5, top right).

4.2 Statistical analysis of collocated measurements

The NO$_2$ profiles retrieved from the SCIAMACHY measurement and those from the HALOE and SAGE II measurements scaled to the SCIAMACHY SZA (Model_occul) were interpolated from the ground to an altitude of 50 km at an 1 km-interval. This facilitates the statistical analysis of the collocated data products, having different vertical resolutions. The dataset of all coincident measurements was divided into subsets of SZA ranges: <40°, 40° to 50°, 50° to 60°, >60°. For each collocation pair the relative deviation, RD, between SCIAMACHY and the HALOE or SAGE measurement scaled to the SCIAMACHY SZA (Model_occul) NO$_2$ concentration was determined at each altitude level (h) using Eq. (1):

$$RD(h) = \frac{SCIAMACHY[NO_2]h - Model\_occul[NO_2]h}{Model\_occul[NO_2]h} \quad (1)$$

For each subset at each altitude level the mean relative deviation (MRD) and root mean square (RMSRD) of the relative deviations between all SCIAMACHY and HALOE measurements scaled to the SCIAMACHY SZA, and SCIAMACHY and SAGE II measurements scaled to the SCIAMACHY SZA were determined. In addition, mean profiles and standard deviations of the profiles for both instruments were calculated for each subset.

Statistical results of the NO$_2$ comparisons from SCIAMACHY with scaled HALOE measurements for the different subsets in dependence to the SCIAMACHY SZA show a MRD between 22 km and 33 km varying from −10 to +12% at SZAs larger than 60° and from −7 to +20% at the SZA range 50° to 60° (Table 1). The RMSRD ranges from 8% to 35% at the SZA between 50° to 60° and from 15% to 25% at SZAs larger than 60°. For the subsets of SCIAMACHY SZA from 40° to 50° and 50° to 60°, good agreement between the HALOE and SCIAMACHY data products extends down to 20 km. Lowest values of MRD of SCIAMACHY to the scaled HALOE measurements are found around 22 km. From this altitude MRDs continuously increase with increasing altitude. Agreement is best at SZA >60° where probably also the largest number of collocations yields a more consistent and meaningful statistical result. For all collocations SCIAMACHY's MRD to the scaled HALOE NO$_2$ measurements varies from −7% to +12% with a RMSRD of 10% to 30% between 21 and 33 km.

Figure 6 shows the statistical results of the NO$_2$ comparisons of data products from SCIAMACHY, HALOE and SAGE II in the high northern latitudes at SZA above 60°. The SCIAMACHY mean profiles are lower at the peak but higher at the upper and lower end of the profile in comparison to scaled HALOE NO$_2$ mean values (Fig. 6, top left); between 18 km and 33 km differences between the two are within the standard deviation of the mean profiles. The MRDs vary between 21 km and 34 km between ±13% with a standard deviation of 15 to 30% (Fig. 6, bottom left). In

contrast, as seen before in the single comparisons, the SCIAMACHY mean profile is systematically lower between 15 and 32 km than the mean of the scaled SAGE II profiles (Fig. 6, top right); between 20 km and 38 km SCIAMACHY shows a negative bias of 10 to 35% with a rather low RMSRD of 5 to 14% in comparison to the scaled SAGE II values (Fig. 6, bottom right). The negative bias increases systematically from 35 km with decreasing altitude. The low RMSRD of SCIAMACHY NO$_2$ values compared to scaled SAGE values may result from the homogenous sample of matches. These were all from a two weeks time period in September, from high northern latitudes, at SCIAMACHY SZA between 60° and 70°, and the SAGE NO$_2$ measurements taken during sunset.

5 Conclusions

The objective of this study is to validate the NO$_2$ profiles retrieved from SCIAMACHY (SCIAMACHY-IUP NO$_2$ profiles V1) by comparison with those retrieved from the measurement of the occultation instruments HALOE and SAGE II. As the measurements are taken at different SZA, and NO$_2$ has a significant diurnal variation, comparison of the collocated measurements, without accounting for the diurnal variation of NO$_2$, is of limited value. We take the following approach:

1. the identification of collocation measurements,

2. the calculation of the amount of NO$_2$ expected at the SZA of SCIAMACHY, based on that determined from the occultation measurement,

3. comparison of the profiles at the same SZA.

The calculation used a photochemical model, initialised with the occultation NO$_2$ and O$_3$ data products and accounting for the photolysis and chemistry of NO$_2$.

A sensitivity analysis of the 1D-photochemcial model, used in the study, indicates that the approach taken in this study appears to be an effective and reliable way to compare collocated NO$_2$ measurements at different SZA between 20 km and 40 km altitude and for day-time measurements. The largest contributions to the overall uncertainity of the model are the O$_3$ profile, knowledge and variation of the SZA along the LOS of the occultation measurement, and the NO$_2$ photolysis rate. Initialising the model with the O$_3$ profile from the occultation measurement rather than using climatological values, not surprisingly, minimises the uncertainty on the knowledge of the calculated NO$_2$ profile at the SCIAMACHY SZA. This was done in our validation of SCIAMACHY NO$_2$ profiles with HALOE and SAGE II measurements and for the comparisons with HALOE the retrieval of NO$_2$ profiles was corrected for SZA variations
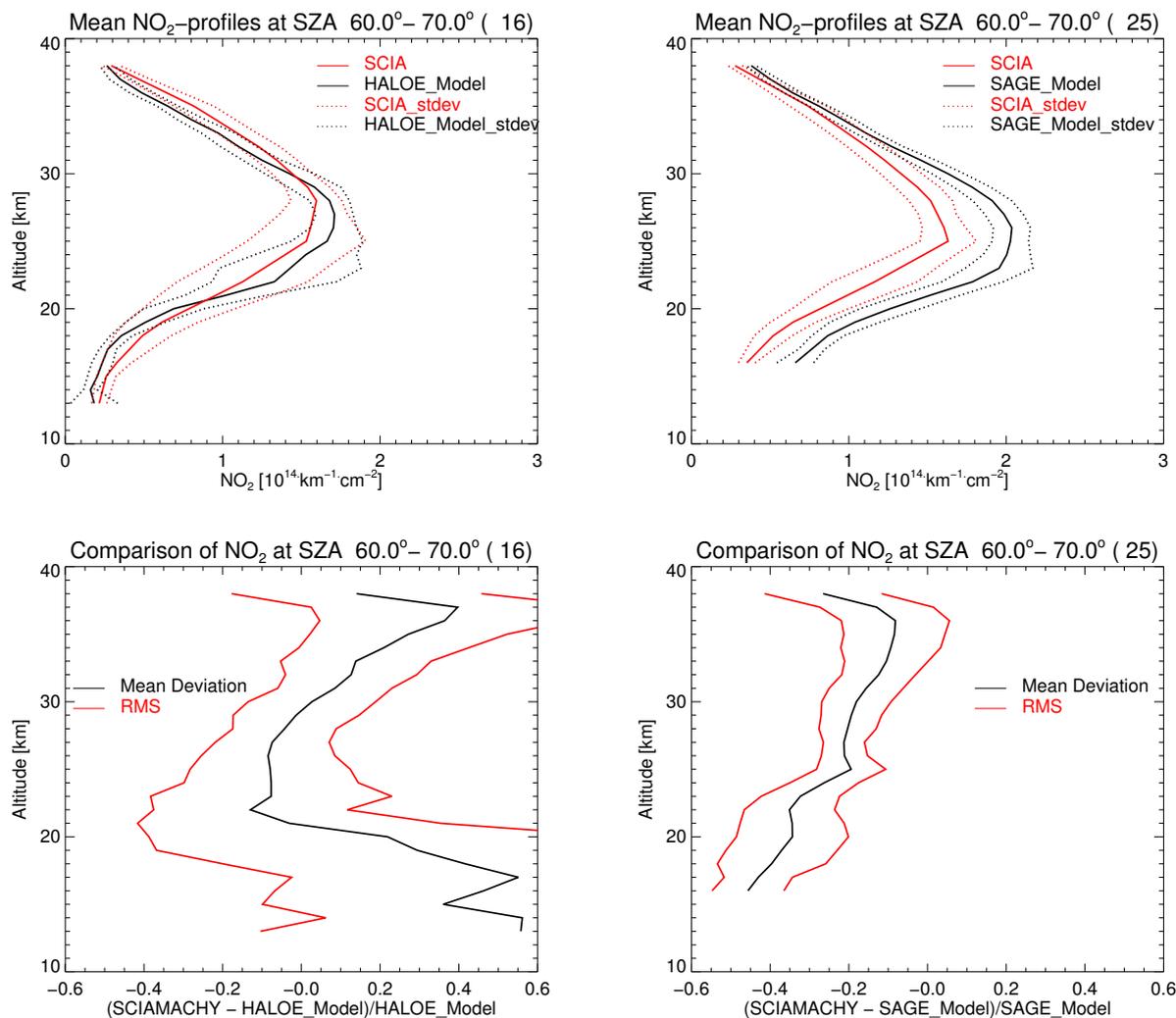
Fig. 6. Statistical results of the comparisons of NO$_2$ profiles from collocated HALOE and SCIAMACHY (top and bottom left) and SAGE and SCIAMACHY (top and bottom right) at the high northern latitudes (55° N to 69° N) at SCIAMACHY SZA between 60° and 70°. All SAGE measurements were taken during sunset. Five HALOE measurements were taken during sunset and eleven during sunrise. At the top the mean NO$_2$ profiles (straight line) and their standard deviation (dotted line) of all SCIAMACHY measurements (red) and the HALOE measurement scaled by the model described in Sect. 3 to the SCIAMACHY SZA (HALOE_Model, black) is shown on the left side, the same for the SCIAMACHY (black) and SAGE (SAGE_Model, red) comparison on the right. The bottom graphs show the mean relative deviation (Mean Deviation, black) and the root mean square of the mean relative deviation (RMS) of all comparisons of NO$_2$ values from SCIAMACHY to HALOE_Model (left) and to SAGE_Model (right) at the respective altitude.

along the LOS. Applying both criteria, the model uncertainty decreases at 20 to 40 km from between 8 and 14% to a value of less than 5%.

The analysis of the model further showed that during the night, besides the O$_3$ profile and the SZA along the LOS of the occultation measurement, the temperature plays a large role in determining the NO$_2$ profile. The overall uncertainty is much larger with about 20% between 15 km and 40 km, rising sharply to over 30% above 40 km, but can be reduced to less than 14% when the O$_3$ profiles are taken from the occultation measurements and retrieval of NO$_2$ profiles is cor-

rected for SZA variations along the LOS. Thus the validation of night-time measurements, from GOMOS stellar occultation, MIPAS limb and SCIAMACHY lunar occultation measurements, with occultation measurements has an intrinsically lower accuracy than that for day-time measurements, unless measurements are made simultaneously.

The validation results presented in this study show a good agreement (within ±12%) between SCIAMACHY and HALOE NO$_2$ profiles from July to October 2002 in the altitude range between 22 and 33 km. The rather large RM-SRD up to 30% of SCIAMACHY to HALOE are attributed

to the heterogeneous sample of collocations, covering the latitudes from 69° N to 65° S and SCIAMACHY SZA from 35° to 69°. The comparison of all SCIAMACHY and SAGE II collocated NO$_2$ profiles show a systematic negative offset between 20 km and 38 km between 10% and 35%, decreasing with increasing altitude. As a result of the homogenous sample for the statistical analysis where all collocations are from the same region at the same SCIAMACHY SZA, the RMSRD of this offset is quite small ($<$15%). This negative offset is attributed to the SAGE II v6.2 NO$_2$ values being too high, because in the comparison of collocated SCIAMACHY, HALOE, and SAGE II NO$_2$ measurements, the scaled SAGE II measurement are high and larger than for the scaled HALOE measurement at all altitudes. This conclusion is supported by the study of Newchurch and Ayoub (2004), where SAGE II sunset NO$_2$ data product from data version 6.0 showed higher values compared to the former versions of SAGE II, v5.931 and v5.96, ATMOS v3.1 and HALOE v19.

In summary, this study has provided a validation of the SCIAMACHY IUP NO$_2$ profiles V1 by comparison with SAGE II and HALOE measurements. This retrieval uses the SCIAMACHY limb measurements of radiation scattered by the atmosphere in the spectral range 420–455 nm. Overall it indicates that SCIAMACHY limb measurements yield significant valuable information during the day about NO$_2$ in the stratosphere. The accuracy is already such that the data are useful for scientific studies. As the knowledge of the instrumental effects and biases improves, and/or by using a larger spectral window, it is expected that the accuracy of the data will somewhat improve.

Edited by: U. Platt

References

Abrams, M. C., Chang, A. Y., Gunson, M. R., Abbas, M. M., Goldman, A., Irion, F. W., Michelsen, H. A., Newchurch, M. J., Rinsland, C. P., Stiller, G. P., and Zander, R.: On the assessment and uncertainty of atmospheric trace gas burden measurements with high resolution infrared solar occultation spectra from space by the ATMOS experiment, Geophys. Res. Lett., 23, 2337–2340, 1996.

Bacmeister, J. T., Kuell, V., Offermann, D., Riese, M., and Elkins, J. W.: Intercomparison of satellite and aircraft observations of ozone, CFC-11, and NO$_y$ using trajectory mapping, J. Geophys. Res., 104, D13, 16 379–16 390, 1999.

Bovensmann, H., Burrows, J. P., Buchwitz, M., Frerick, J., Noël, S., Rozanov, V. V., Chance, K. V., and Goede, A. H. P.: SCIAMACHY – Mission Objectives and Measurement Modes, J. Atmos Sci., 56, 125–150, 1999.

Bertaux, J. L., Megie, G., Widemann, T., Chassefiere, E., Pellinen, R., Korylla, E., Korpela, S., and Simon, P.: Monitoring of Ozone Trend by Stellar Occultations: The Gomos Instrument, Adv. Space Res., 11, 237–242, 1991.

Bracher, A., Weber, M., Bramstedt, K., and Burrows, J. P.: Long-term global measurements of ozone profiles by GOME validated with SAGE II considering atmospheric dynamics, J. Geophys. Res., 109, D20308, doi:10.1029/2004JD004677, 2004.

Brasseur, G. and Solomon, S.: Aeronomy of the Middle Atmosphere, Atmos. Sci. Lib., D. Reidel, Norwell, Mass., 1986.

Chipperfield, M.: Multiannual Simulations with a three-dimensional Chemical Transport Model, J. Geophys. Res., 104, 1781–2805, 1999.

Chu, W. P. and McCormick M. P.: SAGE Observations of Stratospheric Nitrogen Dioxide, J. Geophys. Res., 91, 5465–5476, 1986.

Cunnold, D. M., Zawodny, J. M., Chu, W. P., Pommereau, J. P., Goutail, F., Lenoble, J., McCormick, M. P., Veiga, R. E., Murcray, D., Iwagami, N., Shibasaki, K., Simon, P. C., and Peetermans, W.: Validation Of SAGE II NO$_2$ Measurements, J. Geophys. Res., 96, 12 913–12 925, 1991.

Danilin, M. Y., Ko, M. K. W., Bevilacqua, R. M., Lyjak, L. V., Froidevaux L., Santee, M. L., Zawodny, J. M., Hoppel, K. W., Richard, E. C., Spackman, J. R., Weinstock, E. M., Herman, R. L., McKinney, K. A., Wennberg, P. O., Eisele, F. L., Stimpfle, R. M., Scott, C. J., Elkins, J. W., and Bui, T. V.: Comparison of ER-2 Aircraft and POAM-III, MLS, and SAGE-II satellite measurements during SOLVE using traditional correlative analysis and trajectory hunting technique, J. Geophys. Res., 107, 8315, doi:101029/2002JD000781, 2002.

DeMoore, W. B., Sander, S. P., Golden, D. M., Hampson, R. F., Kurylo, M. J., Howard, C. J., Ravishankara, A. R., Kolb, C. E., and Molina, M. J.: Chemical kinetics and photochemical data for use in stratospheric modelling, Evaluation Number 12, JPL Publication 97-4, Jet Propulsion Laboratory, California Institute of Technology, Pasadena, CA, 1997.

Eichmann, K.-U., Kaiser, J. W., von Savigny, C., Rozanov, A., Rozanov, V. V., Bovensmann, H., Sinnhuber, M., and Burrows, J. P.: The SCIAMACHY limb measurements in the UV/VIS spectral region: first results, Adv. Space Res., 34, 775–779, 2004.

Glaccum, W., Lucke, R., Bevilacqua, R. M., Shettle, E. P., et al.: The Second Polar Ozone and Aerosol Measurement (POAM II) Instrument, J. Geophys. Res., 101, 14 479–14 487, 1996.

Gordley, L. L., Russell III, J. M., Mickley, L. J., Frederick, J. E., Park, J. H., Stone, K. A., Beaver, G. M., McInerney, J. M., Deaver, L. E., Toon, G. C., Murcray, F. J., Blatherwick, R. D., Gunson, M. R., Abbatt, J. P. D., Mauldin III, R. L., Mount, G. H., Sen, B., and Blavier, J. F.: Validation of nitric oxide and nitrogen dioxide measurements made by the Halogen Occultation Experiment for UARS plaform, J. Geophys. Res., 101, 10 241–10 266, 1996.

Harder, H., Bösch, H., Camy-Peyret, C., Chipperfield, M. P., Fitzenberger, R., Payan, S., Perner, D., Platt, U., Sinnhuber, B.-M., and

Pfeilsticker, K.: Comparison of measured and modeled stratospheric BrO: Implications for the total amount of bromine, Geophys. Res. Lett., 27, 3695–3698, 2000.

Hoerling, M. P., Schaak, T. K., and Lenzen, A. J.: Global objective tropopause analyses, Mon. Weather Rev., 119, 1816–1831, 1991.

Kinnersley, J. S.: The meteorology of the stratospheric "THIN AIR" model, Q. J. R. Meteorol. Soc., 122, 219–252, 1996.

Lu, C.-H., Yue, G. K., Manney, G. L., Jäger, H., and Mohen, V. A.: Langrangian approach for Stratospheric Aerosol and Gas Experiment (SAGE) II profile intercomparisons, J. Geophys. Res., 105, 4563–4572, 2000.

Lucke, R. L., Korwan, D., Bevilacqua, R. M., Hornstein, J. S., Shettle, E. P., Chen, D. T. Daehler, M., Lumpe, J. D., Fromm, M. D., Debrestian, D., Neff, B., Squire, M., König-Langlo, G., and Davies, J.: The Polar Ozone and Aerosol Measurement (POAM III) Instrument and Early Validation Results, J. Geophys. Res., 104, 18 785–18 799, 1999.

Marchand, M., Bekki, S., Denis, L., Pommereau, J.-P., and Khattatov, B. V.: Test of the night-time polar stratospheric NO$_2$ decay using wintertime SAOZ measurements and chemical data assimilation, Geophys. Res. Lett., 30, 1920, doi:10.1029/2003GL017582, 2003.

Marchand, M., Bekki, S., Hauchecorne, A., and Bertaux, J.-L.: Validation of the self-consistency of GOMOS NO3, NO2 and O3 data using chemical data assimilation, Geophys. Res. Lett., 31, L10107, doi:10.1029/2004GL019631, 2004.

Mauldin, L. E., Zaun, N. H., McCormick, M. P., Guy, J. J., and Vaughn, W. R.: Stratospheric Aerosol and Gas Experiment II Instrument: A Functional Description, Opt. Eng., 24, 307–312, 1985.

Nasa Langley Research Center: SAGE III – The Stratospheric Aerosol and Gas Experiment III, SAGE III instrument, http://www-sage3.larc.nasa.gov/instrument/, 2004.

Nakajima, H., Sugita, T., Yokota, T., and Sasano, Y.: Current status and early result of the ILAS-II onboard the ADEOS-II satellite, Proceedings of SPIE, Vol. 5234, edited by: Meynart, R., Neeck, S. P., Shimoda, H., Lurie, J. B., and Aten, M. L., pp. 36–45, 2004.

Newchurch, M. J., Allen, M., Gunson, M. R., Salawitch, R. J., Collins, G. B., Huston, K. H., Abbas, M. M., Abrams, M. C., Chang, A. Y., Fahey, D. W., Gao, R. S., Irion, F. W., Lowenstein, M., Manney, G. L., Michelsen, H. A., Podolske, J. R., Rinsland, C. P., and Zander, R.: Stratospheric NO and NO$_2$ abundances from ATMOS solar-occultation measurements, Geophys. Res. Lett., 23, 2372–2376, 1996.

Newchurch, M. and Ayoub, M.: Comparison of the SAGE II version 6.0 measuremetns of NO$_2$ with ATMOS 3.1 and HALOE v19, http://vortex.nsstc.uah.edu/atmchem/strat_no2/main.html, 2004.

Payan, S., Camy-Peyret, C., Jeseck, P., Hawat, T., Pirre, M., Renard, J.-B., Robert, C., Levevre F., Kanzawa, H., and Sasano, Y. S.: Diurnal and nocturnal distribution of stratospheric NO$_2$ from solar and stellar occultation measurements in th Arctic vortex: comparison with models and ILAS satellite measurements, J. Geophys. Res., 104, 21 585–21 593, 1999.

Randall, C. E., Lumpe, J. D., Bevilacqua, R. M., Hoppel, K. W., Shettle, E. P., Rusch, D. W., Gordley, L. L., Kreher, K., Pfeilsticker, K., Boesch, H., Toon, G., Goutail F., and Pommereau, J.-P.: Validation of POAM III NO$_2$ measurements, J. Geophys. Res., 107, 4432, doi:10.1029/2001JD001520, 2002.

Roscoe, H. K., Drummond, J. R., and Jarnot, R. F.: Infrared measurements of stratospheric composition. III. The daytime changes of NO and NO$_2$. Proc. R. Soc. Lond., A375, 507–528, 1981.

Rozanov, A., Rozanov, V., and Burrows, J. P.: A numerical radiative transfer model for a spherical planetary atmosphere: Combined differential – integral approach involving the Picard iterative approximation, J. Quant. Spectrosc. Rad. Transfer, 69, 451–512, 2001.

Russell III, J. M., Gordley, L. L., Gordley, J. H., Park, J. H., Drayson, S. R., Hesketh, W. D., Cicerone, R. J., Tuck, A. F., Frederick, J. E., Harries, J. E., and Crutzen, P. J.: The Halogen Occultation Experiment, J. Geophys. Res., 98, 10 777–10 797, 1993.

Sander, S. P., Friedl, R. R., DeMore, W. B., Golden, D. M., Kurylo, M. J., Hampson, R. F., Huie, R. E., Moortgat, G. K., Ravishankara, A. R., Kolb, C. E., and Molina, M. J.: Chemical kinetics and photochemical data for use in stratospheric modeling, Evaluation Number 13, JPL Publication 00-3, Jet Propulsion Laboratory, California Institute of Technology, Pasadena, CA, 2000.

Sasano, Y., Suzuki, M., and Yokota, T.: Improved Limb Atmospheric Spectrometer (ILAS) for stratospheric ozone layer measurements by solar occultation technique, Geophys. Res. Lett., 26, 197–200, 1999.

von Savigny, C., Rozanov, A., Bovensmann, H., Eichmann, K.-U., Kaiser, J. W., Noël, S., Rozanov, V. V., Sinnhuber, B.-M., Weber, M., and Burrows, J. P.: The Ozone hole break-up in September 2002 as seen by SCIAMACHY on ENVISAT. J. Atmosph. Sci., accepted, 2004.

Sinnhuber, B.-M., Arlander, D. W.. Bovensmann, H. , Burrows, J. P., Chipperfield, M. P. , Enell, C.-F., Frieß, U., Hendrick, F., Johnston, P. V., Jones, R. L., Kreher, K., Mohamed-Tahrin, N., Müller, R., Pfeilsticker, K., Platt, U., Pommereau, J.-P., Pundt, I., Richter, A., South, A. M., Tørnkvist, K. K., Van Roozendael, M., Wagner, T., and Wittrock, F.: Comparison of measurements and model calculations of stratospheric bromine monoxide, J. Geophys. Res., 107, doi:10.1029/2001JD000940, 2002.

Sinnhuber M., Burrows, J. P., Chipperfield, M. P., Jackman, C. H., Kallenrode, M.-B., Künzi, K., and Quack, M.: A model study of the impact of magnetic field structure on atmospheric composition during solar proton events, Geophys. Res. Lett., 2003GL017265, 2003.

Solomon, S. and Keys, J. G.: Seasonal variations in Antarctic NO$_x$ chemistry, J. Geophys. Res., 88, 5229–5239, 1992.

Stiller, G. P., Glatthor, N., Kellmann, S., Kimmich, E., Linden, A., Milz, M., and Fischer, H.: MIPAS on ENVISAT as an UT/LS Sounder, in: IRS 2000, edited by: Smith, W. L. and Timofeyev, Yu M., Current Problems in Atmospheric Radiation, A. Deepak Publishing, Hampton, Virginia, 839–842, 2001.

Stowasser, M., Oelhaf, H., Ruhnke, R., Kleinert, A., Wetzel, G., Friedl-Vallon, F., Kouker, W., Lengel, A., Maucher, G., Nordmeyer, H., Reddmann, T., and Fischer, H.: The variation of short-lived NO$_y$ species around sunrise at mid-latitudes as measured by MIPAS-B and calculated by KASIMA, Geophys. Res. Lett., 30, 1432, doi:10.1029/2002GL016272, 2003.

Swinbank, R. and O'Neill, A.: A Stratosphere-Troposphere Data Assimilation System, Mon. Weather Rev., 122, 686–702, 1994.

Vogel, B., Müller, R., Deshler, T., Grooß, J.-U., Karhu, J., McKenna, D. S., Müller, M., Toohey, D., Toon, G. C., and

Stroh, F.: Vertical profiles of activated ClO and ozone loss in the Arctic vortex in January and March 2000: In situ observations and model simulations, J. Geophys. Res., 108, 8334, doi:10.1029/2002JD002564, 2003.

Weber, M., Dhomse, S., Wittrock, F., Richter, A., Sinnhuber, B.-M., and Burrows, J. P.: Dynamical control of NH and SH winter/spring total ozone from GOME observations in 1995–2002, Geophys. Res. Lett., 30, 1853, doi:10.1029/2002GL016799, 2003.